

Constraints between concurrence and polarization for mixed states subjected to open system dynamics

Y. Yusra , C. Montenegro , and F. De Zela 

Departamento de Ciencias, Sección Física, Pontificia Universidad Católica del Perú, Apartado 1761, Lima, Peru



(Received 25 November 2021; accepted 31 May 2022; published 10 June 2022)

Entanglement and polarization are mutually constrained by the relationship $C^2 + P^2 = 1$, which engages the concurrence C of a pure, two-qubit state and the degree of polarization P of either of its two subsystems. How the above constraint generalizes for mixed states is an open question. We address mixed, two-qubit states of the X type, i.e., those whose density matrix has nonzero elements only in the two main diagonals. We focus on mixed states that arise out of a pure, two-qubit state that is subjected to either the amplitude damping channel or the depolarizing channel. We derive alternative constraints for concurrence and polarization and test them experimentally with polarization-entangled photons. We argue that our theoretical results hold also for classical light, whenever two binary degrees of freedom can be entangled.

DOI: [10.1103/PhysRevA.105.063710](https://doi.org/10.1103/PhysRevA.105.063710)

I. INTRODUCTION

For years, entanglement was viewed as the most distinctive feature of quantum mechanics, a feature that was seemingly in conflict with local realism. In the course of time, though, such a view gradually changed. More and more people noticed that entanglement is actually defined solely in terms of linear algebraic properties of vector spaces [1]. These spaces, in turn, can be used to describe either quantum or classical phenomena. In classical optics, for instance, one often deals with light beams whose electric field has multiple degrees of freedom (DOFs), e.g., those referring to space, time, and polarization. If one has independent access to these DOFs, their proper mathematical description requires making use of a tensor-product vector space. It is then possible to deal with entangled states that violate the Bell-Cluser-Horne-Shimony-Holt inequality [2,3], similarly to what happens in standard, quantum Bell tests. Another feature that can appear in both classical and quantum phenomena is polarization. Its original formulation referred to a particular case: the polarization of a plane wave's electric field. This field can be described as a coherent superposition of two vectors. The correlation between the amplitudes of these two vectors can be quantified with a basis-dependent measure, the so-called “degree of coherence” [4]. A basis-independent measure, the degree of polarization P , can be defined as the maximum degree of coherence over all orthonormal bases [5]. As for entanglement, a basis-independent measure is, for instance, concurrence C [6]. It turns out that the two measures, P and C , can be related to one another. Indeed, as was recently shown [7], the degree of entanglement of a pure, two-qubit system and the degree of polarization of either of its one-qubit subsystems are mutually constrained, according to the equality

$$C^2 + P^2 = 1. \quad (1)$$

Equation (1) might seem somewhat counterintuitive, because C , a quantity that involves the two subsystems, turns out to be linked to P , which measures a property that each (sub)system can have, irrespective of the other one. However, (1) makes sense when we recall that a system cannot be in a pure state if it is entangled with another system. The pure, two-qubit state, to which (1) refers, can be written as

$$|\Phi_{AB}\rangle = \alpha_1|00\rangle + \alpha_2|01\rangle + \alpha_3|10\rangle + \alpha_4|11\rangle, \quad (2)$$

with $\sum_i |\alpha_i|^2 = 1$. The marginal density operators of the two subsystems, $\rho_A = \text{Tr}_B(|\Phi_{AB}\rangle\langle\Phi_{AB}|)$ and $\rho_B = \text{Tr}_A(|\Phi_{AB}\rangle\langle\Phi_{AB}|)$, can be expressed in terms of the identity matrix I and the triple of Pauli matrices, $\sigma = (\sigma_1, \sigma_2, \sigma_3)$, as

$$\rho_k = \frac{1}{2}(I + \mathbf{S}_{(k)} \cdot \sigma) \equiv \frac{1}{2}(I + P \hat{\mathbf{n}}_{(k)} \cdot \sigma), \quad k = A, B. \quad (3)$$

Here, $\mathbf{S}_{(k)}$ are Stokes (or Bloch) vectors, and $P = |\mathbf{S}_{(k)}|$ is the degree of polarization. Equation (1) follows from expressing C in terms of the purities of each subsystem [8]: $C = \sqrt{2(1 - \text{Tr}\rho_A^2)} = \sqrt{2(1 - \text{Tr}\rho_B^2)}$. Indeed, Eq. (3) gives $\text{Tr}\rho_A^2 = \text{Tr}\rho_B^2 = (1 + P^2)/2$, so that (1) immediately follows. As remarked in Ref. [7], the relationship between C and P , given by Eq. (1), “is significant, not coincidental.” We may naturally ask how significant it is. How are concurrence and polarization related to one another when we have a mixture ρ_{AB} instead of a pure state $|\Phi_{AB}\rangle$? This question still remains wide open. In the case of pure states, Eq. (1) can be understood as a complementarity relation, one which may engage different pairs of coherences [7]. If some of these coherences are “hidden” in an optical beam, the projection of all but two of the beam's DOFs makes accessible the mutual coherence that the remaining pair may have [7]. In the case of mixed states, we deal with open systems. The system's environment may play different roles, possibly giving rise to various complementarity relations that extend the one given by Eq. (1). Coherence can in turn be understood as the ability to interfere

[4], which brings in concepts such as visibility V and distinguishability D . One can then arrive at a “trality relation” [9] that reads $D^2 + V^2 + C^2 = 1$. This is one among several relations that can be established [10–13]. These relations have shed light on one of the quintessential aspects of quantum mechanics: wave-particle duality. In it, coherence plays a central role. Moreover, when considering two subsystems of a whole system, it can happen that coherence appears as a property of the latter and only partially as a property of each subsystem. Partial coherence can thus migrate from one subsystem to the other, thereby becoming hidden. By submitting the whole system to appropriate, global unitary transformations, one can make hidden coherences available again [14].

In the case of mixed states, concurrence is defined [6] in terms of $\tilde{\rho}_{AB} = (\sigma_2^A \otimes \sigma_2^B) \rho_{AB}^* (\sigma_2^A \otimes \sigma_2^B)$, where ρ_{AB}^* is a matrix whose entries are the complex conjugates of ρ_{AB} , when the latter is written in the computational basis. Concurrence is then given by $C = \max\{0, \sqrt{\lambda_1} - \sqrt{\lambda_2} - \sqrt{\lambda_3} - \sqrt{\lambda_4}\}$, where $\lambda_1, \dots, \lambda_4$ are the eigenvalues of $\rho_{AB} \tilde{\rho}_{AB}$ in decreasing order. While the “spin-flip” effect $\rho_k \rightarrow \sigma_2 \rho_k^* \sigma_2 = (I - P \hat{\mathbf{n}}_{(k)} \cdot \boldsymbol{\sigma})/2$ still connects $\tilde{\rho}_{AB}$ with polarization, the incidence of $\rho_{AB} \tilde{\rho}_{AB}$ in C makes the connection between concurrence and polarization much more involved, provided there is such a connection in the most general case. To be sure, one can formally connect entanglement and polarization by resorting to the entanglement of formation [15]

$$E_f(\rho_{AB}) = \min \sum_i p_i E(\psi_i^{AB}). \quad (4)$$

Here, the minimization is taken over all pure-state decompositions of the mixed state: $\rho_{AB} = \sum_i p_i |\psi_i^{AB}\rangle \langle \psi_i^{AB}|$. The pure-state entanglement measure $E(\psi_i^{AB})$ is given by [6]

$$E(\psi_i^{AB}) = h\left(\frac{1 + \sqrt{1 - C^2(\psi_i^{AB})}}{2}\right) = h\left(\frac{1 + P_i}{2}\right), \quad (5)$$

where $h(x) = -x \log_2 x - (1-x) \log_2 (1-x)$ is the binary entropy function and we have used (1) in the second step. Hence we can write $E_f(\rho_{AB})$ in terms of the P_i instead of the $C(\psi_i^{AB})$. This was done in Ref. [16], where Eq. (1) was anticipated. However, what we are seeking for is an explicit, closed-form expression that involves a single degree of polarization and concurrence, or any other entanglement measure. This would bring us closer to answering the question about the significance of (1), as a relation between entanglement and polarization.

When the bipartite state ρ_{AB} is mixed, i.e., $\text{Tr} \rho_{AB}^2 < 1$, one expects that (1) is replaced by the inequality

$$C^2 + P_k^2 \leq 1, \quad k = A, B. \quad (6)$$

The respective degrees of polarization of the two subsystems are now, in general, $P_A \neq P_B$. To the best of our knowledge, inequality (6) has been proved only for a class of mixed states, the so-called X states [17]. This class contains several subclasses of mixed states, such as partially entangled states, e.g., Werner states [18], as well as nonentangled states [19]. In this paper, we address a class of X states that are experimentally accessible with linear optics. As we shall see, for X states one can derive the inequality (6). It is also possible to

obtain some equalities that generalize the constraint given by Eq. (1). Al-Qasimi has recently reported such an equality [17], which is similar—and, in one case, identical—to the ones we report here. However, while Al-Qasimi’s treatment focuses on classical optical beams, ours embraces both classical and single-photon beams. Our study should give further support to viewing entanglement as a property that is not restricted to quantum phenomena. Indeed, “entanglement is becoming widely understood to be present in classical as well as in quantum physics, with notable examples already appearing in optical studies, both classical and quantum” [20]. As we said before, the very definition of entanglement applies whenever we deal with the tensor product of two vector spaces, irrespective of the classical or quantum nature of the physical entities being described by those vector spaces [2,21–28]. Hence, while the experiments we report were conducted with single photons, the same results should be obtained with analogous experiments that are conducted using classical light beams. What matters is that two DOFs can get entangled and that each of these DOFs can be represented by a qubit. C and P can then be defined as above, and their constraints will manifest themselves, no matter which physical realization of the DOFs one uses, classical or quantum.

II. X STATES

X states are characterized by the form of their density matrix in the computational basis:

$$\rho_X = \begin{pmatrix} a & 0 & 0 & w \\ 0 & b & z & 0 \\ 0 & z^* & c & 0 \\ w^* & 0 & 0 & d \end{pmatrix}. \quad (7)$$

The square roots of the eigenvalues of $\rho_X \tilde{\rho}_X$ are $|\sqrt{ad} \pm |w||$ and $|\sqrt{bc} \pm |z||$. As can be shown [19], the non-negativity of ρ_X implies that $|z| \leq \sqrt{bc}$ and $|w| \leq \sqrt{ad}$. Thus the largest of the above values is either $|\sqrt{ad} + |w||$ or $|\sqrt{bc} + |z||$. It is then easy to see that, for X states, concurrence, i.e., $C = \max\{0, \sqrt{\lambda_1} - \sqrt{\lambda_2} - \sqrt{\lambda_3} - \sqrt{\lambda_4}\}$, can be written as

$$C = 2 \max\{0, |z| - \sqrt{ad}, |w| - \sqrt{bc}\}. \quad (8)$$

If $C = 2(|z| - \sqrt{ad})$, then, on taking into account that $|z| \leq \sqrt{bc}$, we conclude that $C \leq 2(\sqrt{bc} - \sqrt{ad})$. Similarly, if $C = 2(|w| - \sqrt{bc})$, we conclude that $C \leq 2(\sqrt{ad} - \sqrt{bc})$. Thus $C \leq 2|\sqrt{ad} - \sqrt{bc}|$.

The degrees of polarization $P_k = \sqrt{1 - 4 \text{Det} \rho_k}$ of the trace-1 marginal matrices, $\rho_A = \text{Tr}_B \rho_X$ and $\rho_B = \text{Tr}_A \rho_X$, are given by

$$P_A = \sqrt{1 - 4(a+b)(c+d)}, \quad (9)$$

$$P_B = \sqrt{1 - 4(a+c)(b+d)}. \quad (10)$$

From the foregoing results, it follows that

$$\begin{aligned} C^2 + P_A^2 &\leq 4(\sqrt{ad} - \sqrt{bc})^2 + 1 - 4(a+b)(c+d) \\ &= 1 - 4(\sqrt{ac} + \sqrt{bd})^2 \leq 1, \end{aligned} \quad (11)$$

$$\begin{aligned} C^2 + P_B^2 &\leq 4(\sqrt{ad} - \sqrt{bc})^2 + 1 - 4(a+c)(b+d) \\ &= 1 - 4(\sqrt{ab} + \sqrt{cd})^2 \leq 1. \end{aligned} \quad (12)$$

Thus (6) is proved for general X states (see also Ref. [17]). For some class of X states, inequality (6) can be replaced by a tighter constraint—an equality—as we show next.

A. X states related to the amplitude damping channel

Here, we focus on X states that result from letting an initially pure, two-qubit state evolve into a mixed state. We assume that each qubit is subjected to the action of an environment. This environment acts independently on each qubit and in a way that can be modeled by the amplitude damping channel (ADC) [29]. To fix ideas, we consider two photons being in the pure state

$$|\psi_{AB}\rangle = \cos\theta |H_A\rangle|V_B\rangle + e^{i\phi} \sin\theta |V_A\rangle|H_B\rangle, \quad (13)$$

where H and V refer to horizontal and vertical polarization, respectively. The corresponding density matrix is then given by

$$\rho_{AB}^{(0)} = |\psi_{AB}\rangle\langle\psi_{AB}| = \begin{pmatrix} 0 & 0 & 0 & 0 \\ 0 & \cos^2\theta & e^{-i\phi} \cos\theta \sin\theta & 0 \\ 0 & e^{i\phi} \cos\theta \sin\theta & \sin^2\theta & 0 \\ 0 & 0 & 0 & 0 \end{pmatrix}. \quad (14)$$

The initial state evolves according to

$$\rho_{AB} = \mathcal{E}(\rho_{AB}^{(0)}) = \sum_{\mu=0}^1 \sum_{\nu=0}^1 M_{\mu}^A \otimes M_{\nu}^B (\rho_{AB}^{(0)}) M_{\mu}^{A\dagger} \otimes M_{\nu}^{B\dagger}, \quad (15)$$

where the M_{μ} are Kraus operators that act locally on each qubit, making it undergo a dissipative process which we have

$$\rho_{AB} = \begin{pmatrix} p & 0 & 0 & 0 \\ 0 & (1-p)\cos^2\theta & e^{-i\phi}(1-p)\cos\theta\sin\theta & 0 \\ 0 & e^{i\phi}(1-p)\cos\theta\sin\theta & (1-p)\sin^2\theta & 0 \\ 0 & 0 & 0 & 0 \end{pmatrix}. \quad (21)$$

The marginal density matrices ρ_A and ρ_B have the following degrees of polarization associated with them:

$$P_A = |p + (1-p)\cos 2\theta|, \quad (22)$$

$$P_B = |p - (1-p)\cos 2\theta|. \quad (23)$$

Concurrence is given by

$$C(\rho_{AB}) = (1-p)|\sin 2\theta|. \quad (24)$$

Setting $p = 0$, we recover the values $P_A = P_B = |\cos 2\theta|$ and $C = |\sin 2\theta|$ that correspond to the initial, pure state $\rho_{AB}^{(0)}$, for which Eq. (1) holds true. As can be readily seen from Eqs. (22)–(24), in the case $p > 0$, Eq. (1) generalizes to

$$C_{AB}^2 + (P_A \pm p)^2 = (1-p)^2, \quad (25)$$

$$C_{AB}^2 + (P_B \pm p)^2 = (1-p)^2, \quad (26)$$

where we have slightly changed our notation, setting C_{AB} instead of C , to emphasize that concurrence refers to the

chosen to be the ADC. This process corresponds, e.g., to spontaneous photon emission by a two-level atom. Let us assume that the horizontally polarized state represents the ground state and the vertically polarized state represents the excited state, whereas $|0_E\rangle$ and $|1_E\rangle$ are the vacuum state and one-photon state, respectively, of the environment. The ADC is then given by the map

$$|H_A\rangle|0_E\rangle \rightarrow |H_A\rangle|0_E\rangle, \quad (16)$$

$$|V_A\rangle|0_E\rangle \rightarrow \sqrt{1-p}|V_A\rangle|0_E\rangle + \sqrt{p}|H_A\rangle|1_E\rangle, \quad (17)$$

and similarly for the B subsystem. The parameter p is the probability for the system to make a transition from the excited to the ground state, thereby transferring its energy to the environment. The corresponding Kraus operators that act locally on each subsystem are

$$M_0 = \begin{pmatrix} 1 & 0 \\ 0 & \sqrt{1-p} \end{pmatrix}, \quad M_1 = \begin{pmatrix} 0 & \sqrt{p} \\ 0 & 0 \end{pmatrix}. \quad (18)$$

The experimental implementation of the ADC can be done with an interferometric setup, in which the environmental qubits are realized by the two-way path of, say, Sagnac [30] or Mach-Zehnder [31] interferometers. The ADC map consisting of (16) and (17) may be obtained from the transformation

$$|H_A\rangle|0_E\rangle \rightarrow \cos 2\theta_H |H_A\rangle|0_E\rangle + \sin 2\theta_H |V_A\rangle|1_E\rangle, \quad (19)$$

$$|V_A\rangle|0_E\rangle \rightarrow \cos 2\theta_V |V_A\rangle|0_E\rangle + \sin 2\theta_V |H_A\rangle|1_E\rangle, \quad (20)$$

by setting $\theta_H = 0$ and $\sin^2(2\theta_V) = p$. The above transformation can be easily realized with interferometric setups supplemented with half-wave plates [30].

The evolved state $\rho_{AB} = \mathcal{E}(\rho_{AB}^{(0)})$ has the density matrix

two-qubit system, whereas P_A and P_B refer to one-qubit subsystems. As for the signs \pm in (25) and (26), they depend on the positiveness or negativeness of the expressions within the absolute values in (22) and (23). Equation (25) represents a circumference in the C_{AB} - P_A plane, with radius $1-p$, and similarly for (26). Furthermore, we can connect C_{AB} with the two degrees of polarization in a single equation. Indeed, on noting that $P_B^2 - P_A^2 = 4p(1-p)\cos 2\theta$, we obtain, for $p \neq 0$,

$$(4pC_{AB})^2 + (P_B^2 - P_A^2)^2 = 16p^2(1-p)^2. \quad (27)$$

Equations (25)–(27) generalize the constraint given by Eq. (1). Like the latter, the constraints we have found hint at a significant, not coincidental connection between concurrence and polarization. It is worth noting that the above constraints depend not only on the X state we start with, but also on the evolution this state was submitted to. To see this, we address next another type of evolution.

B. X states related to the depolarizing channel

Let us refer again to Al-Qasimi’s recent results [17], which concern the initial, X-type state

$$|\psi\rangle = \cos\theta|0\rangle|0\rangle + \sin\theta|1\rangle|1\rangle. \quad (28)$$

When submitted to uncorrelated noise, this state evolves to

$$\rho_W = \frac{\epsilon}{4}I + (1 - \epsilon)|\psi\rangle\langle\psi|, \quad (29)$$

with $0 \leq \epsilon \leq 1$. The constraint that can be derived in this case reads [17]

$$\left(C + \frac{\epsilon}{2}\right)^2 + P^2 = (1 - \epsilon)^2. \quad (30)$$

Here, $P = (1 - \epsilon)|\cos 2\theta|$ is the common degree of polarization of the two subsystems, and concurrence, as follows from (8), equals $C = |(1 - \epsilon)\sin 2\theta| - \epsilon/2$ when $C \neq 0$, and zero otherwise.

The constraints we derived before, (25), (26), and (30), restrict the values of concurrence and polarization to lie on circumferences, the radii and centers of which depend on how mixed the corresponding states are, as measured by p and ϵ , respectively. Similarly to the case of (25) and (26), in which mixedness comes from amplitude damping, in the case of (30), mixedness comes from the depolarizing, ϵ -weighted contribution that is associated with I in ρ_W [see (29)]. The process that leads from $\rho_W^{(0)} = |\psi\rangle\langle\psi|$ to ρ_W can indeed be described in terms of a generalization of the depolarizing channel [29]. To see this, we first observe that the two-qubit identity operator I can be expressed as

$$\frac{1}{4}I = \sum_{\mu=0}^3 \sum_{\nu=0}^3 \sigma_{\mu} \otimes \sigma_{\nu} (\rho_W^{(0)})_{\sigma_{\mu}} \otimes \sigma_{\nu}, \quad (31)$$

where σ_0 stands for the one-qubit identity. On replacing (31) in (29), we get

$$\begin{aligned} \rho_W = & \left(1 - \frac{3\epsilon}{4}\right)\rho_W^{(0)} + \frac{\epsilon}{4} \left[\sum_{\nu=1}^3 \sigma_0 \otimes \sigma_{\nu} (\rho_W^{(0)})_{\sigma_0} \otimes \sigma_{\nu} \right. \\ & + \sum_{\mu=1}^3 \sigma_{\mu} \otimes \sigma_0 (\rho_W^{(0)})_{\sigma_{\mu}} \otimes \sigma_0 \\ & \left. + \sum_{\mu=1}^3 \sum_{\nu=1}^3 \sigma_{\mu} \otimes \sigma_{\nu} (\rho_W^{(0)})_{\sigma_{\mu}} \otimes \sigma_{\nu} \right], \quad (32) \end{aligned}$$

which generalizes the depolarizing channel for a single qubit [29]: $\mathcal{E}(\rho) = (1 - 3\epsilon/4)\rho + (\epsilon/4) \sum_{i=1}^3 \sigma_i \rho \sigma_i$.

Thus the process $\mathcal{E}(\rho_W^{(0)})$ that leads from $\rho_W^{(0)}$ to ρ_W has in this case 16 Kraus operators $K_{\mu\nu} \propto \sigma_{\mu} \otimes \sigma_{\nu}$. It is rather difficult to implement such a number of operators with linear optics. However, the same \mathcal{E} can be realized with fewer operators, as we show next.

C. Effective depolarizing channel

For the sake of comparing the depolarizing channel with the ADC, it will be convenient to address the state ρ_W , as given by (29), but with $|\psi_{AB}\rangle$ of Eq. (13) replacing the state (28) that

enters (29). Our aim is thus to get

$$\rho_W = \frac{p}{4}I + (1 - p)|\psi_{AB}\rangle\langle\psi_{AB}|, \quad (33)$$

as the result of an evolution \mathcal{E} that may be implemented with linear optics, similarly to what we have done with the ADC.

For simplicity, we set $\phi = 0$ in $|\psi_{AB}\rangle$ [see Eq. (13)]. Our results concerning concurrence and polarization do not depend on ϕ . The state $|\psi_{AB}\rangle$ can be supplemented with three other ones, so as to get a decomposition of the two-qubit identity operator I in the form

$$I = |\psi_{AB}^+\rangle\langle\psi_{AB}^+| + |\psi_{AB}^-\rangle\langle\psi_{AB}^-| + |\phi_{AB}^+\rangle\langle\phi_{AB}^+| + |\phi_{AB}^-\rangle\langle\phi_{AB}^-|, \quad (34)$$

where we have set $|\psi_{AB}^{\pm}\rangle = |\psi_{AB}\rangle$ with $\phi = 0$. The four states in the above equation read

$$|\psi_{AB}^+\rangle = \cos\theta|H_A\rangle|V_B\rangle + \sin\theta|V_A\rangle|H_B\rangle, \quad (35)$$

$$|\psi_{AB}^-\rangle = \sin\theta|H_A\rangle|V_B\rangle - \cos\theta|V_A\rangle|H_B\rangle, \quad (36)$$

$$|\phi_{AB}^+\rangle = \cos\theta|H_A\rangle|H_B\rangle + \sin\theta|V_A\rangle|V_B\rangle, \quad (37)$$

$$|\phi_{AB}^-\rangle = \sin\theta|H_A\rangle|H_B\rangle - \cos\theta|V_A\rangle|V_B\rangle. \quad (38)$$

These states are maximally entangled (Bell) states for $\theta = \pi/4$. Using the above expressions together with (34) and (33), one can get the following Kraus operators:

$$K_0 = \sqrt{1 - 3p/4} \sigma_0 \otimes \sigma_0, \quad (39)$$

$$K_1 = \sqrt{p/4} \sigma_0 \otimes \sigma_1, \quad (40)$$

$$K_2 = -i\sqrt{p/4} \sigma_1 \otimes \sigma_2, \quad (41)$$

$$K_3 = i\sqrt{p/4} \sigma_2 \otimes \sigma_0. \quad (42)$$

One can check that the completeness relation holds: $\sum_{\mu} K_{\mu}^{\dagger} K_{\mu} = I$, as well as

$$\rho_{AB}^W = \sum_{\mu=0}^3 K_{\mu} (|\psi_{AB}\rangle\langle\psi_{AB}|) K_{\mu}^{\dagger} = \frac{p}{4}I + (1 - p)|\psi_{AB}\rangle\langle\psi_{AB}|. \quad (43)$$

From (43) and using (8)–(10), we can calculate concurrence and polarization. We obtain $C_{AB}^W = (1 - p)|\sin 2\theta| - p/2$ and $P_A = P_B = (1 - p)|\cos 2\theta|$, so that

$$\left(C_{AB}^W + \frac{p}{2}\right)^2 + P_k^2 = (1 - p)^2, \quad k = A, B, \quad (44)$$

holds as long as $C_{AB}^W \neq 0$. Equations (44) and (30) are the same. The latter referred to the state $|\psi\rangle = |\phi_{AB}^+\rangle$. Equation (44) holds in fact for the four states $|\psi_{AB}^{\pm}\rangle, |\phi_{AB}^{\pm}\rangle$.

Hence, regarding concurrence and polarization, the pure state $|\psi_{AB}\rangle$ obeys the constraint given by Eq. (1). If this pure state evolves into a mixed state of the X type, then said constraint changes in a way that depends on the type of evolution. For instance, while the evolution (43) maintains the initial balance in polarization ($P_A = P_B$), the ADC can break it. Furthermore, the ranges within which concurrence and polarizations may initially vary are also differently affected by one or the other evolution. These ranges are fixed by the

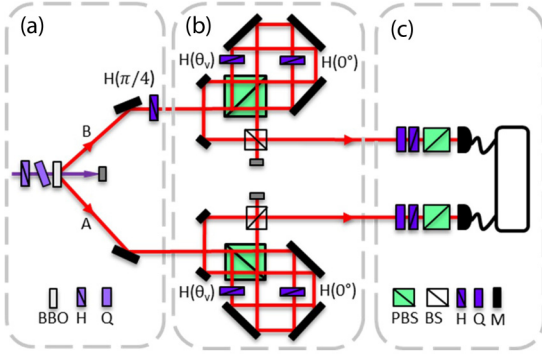


FIG. 1. Experimental setup. (a) Generation of polarization-entangled photons by spontaneous parametric downconversion. (b) Amplitude damping channels implemented with Sagnac-type interferometers. (c) Tomographic two-qubit state characterization. BBO, beta-barium-borate crystals; H, half-wave plate; Q, quarter-wave plate; PBS, polarizing beam splitter; BS, 50 : 50 beam splitter; M, mirror.

different constraints into which (1) changes, as a consequence of the process followed by the initial, pure state.

III. EXPERIMENTAL SETUP AND RESULTS

We tested the constraints we found, Eqs. (25)–(27), by conducting experiments with single photons. More specifically, we produced polarization-entangled photons of 800 nm wavelength by means of spontaneous parametric downconversion (SPDC) in two beta-barium-borate (BBO) crystals, the optical axes of which were oriented perpendicular to one another [32] [see Fig. 1(a)]. The BBO crystals were pumped with a cw laser of 400 nm wavelength (0.7 nm linewidth, 37.5 mW). Each downconverted photon was directed towards a Sagnac-type interferometer, in which the ADC was implemented [see Fig. 1(b)]. In these Sagnac interferometers, the path degree of freedom serves as an ancilla, with the help of which the transformations of Eqs. (19) and (20) can be realized, as already explained. With a half-wave plate and a tilted quarter-wave plate set before the BBO crystals, a state $|\phi_{AB}^+\rangle$ [see Eq. (37)] was produced by SPDC [32]. Thereafter, a half-wave plate set at 45° turned the horizontal polarization of one of these photons into a vertical one, and vice versa, so as to obtain the state $|\psi_{AB}^+\rangle$ [see Eq. (35)]. After being subjected to the ADC to produce the desired X states, the photons were submitted to two-qubit state tomography [see Fig. 1(c)]. The required counting of coincident photon detections was done with synchronized avalanche photodetectors, the coincidence window of which was 10.42 ns. We applied the standard tomographic procedure of James *et al.* [33]. Having determined the density matrix of the state, we extracted from this matrix the desired parameters: C_{AB} , P_A , and P_B , as well as purity, $\mathcal{P} = (4/3)(\text{Tr} \rho^2 - 1/4)$, and fidelity, $\mathcal{F}(\rho, \rho_{\text{exp}}) = \text{Tr}[\sqrt{\rho^{1/2} \rho_{\text{exp}} \rho^{1/2}}]$.

In Fig. 2, we show two examples of our tomographic outputs. One example corresponds to the initial, pure state $|\psi_{AB}^+\rangle = \cos \theta |H_A\rangle |V_B\rangle + \sin \theta |V_A\rangle |H_B\rangle$ (two upper panels), and the other example corresponds to the result of having submitted the pure state to the action of ADCs, so as to produce

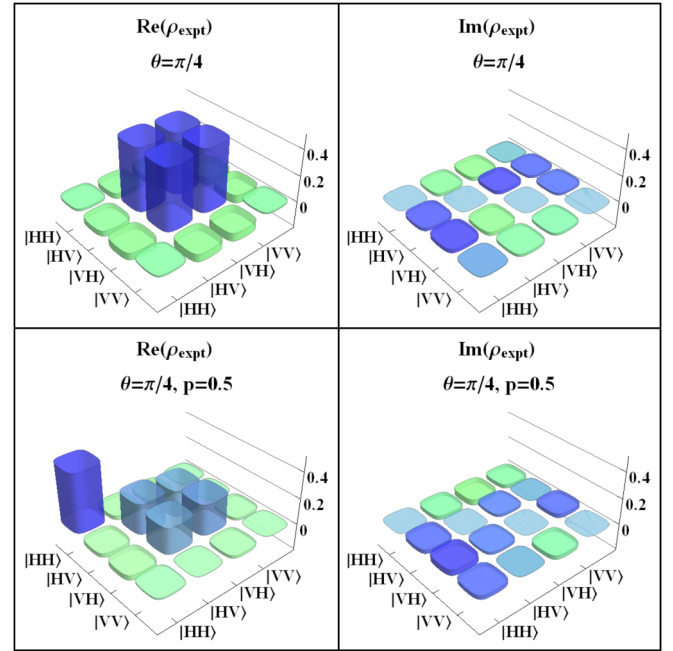


FIG. 2. Real and imaginary parts of the density matrix of a pure state $|\psi_{AB}^+\rangle$ (upper panels) and a mixed, X -type state (lower panels). The measured purity of $|\psi_{AB}^+\rangle$ was 91%, and its fidelity was 0.950 ± 0.001 . The fidelity of the X state was 0.904 ± 0.035 .

a mixed, X state (two lower panels). The purity of $|\psi_{AB}^+\rangle$ was 91%, and its fidelity was 0.950 ± 0.001 . As for the X state, its fidelity was 0.904 ± 0.035 . These were typical values for our measurements. Our experimental outcomes for concurrence and polarization had an accuracy that was consistent with those values.

In Fig. 3, we show our measurements of C_{AB} , P_A , and P_B as parametric functions of the angle θ that specifies the initial state $|\psi_{AB}^+\rangle$. We considered three X states. One of them, with $p = 0$, corresponds to the initial, pure state $|\psi_{AB}^+\rangle$, and the other two cases correspond to setting $p = 0.5$ and 0.75 in Eqs. (25) and (26). These equations are the constraints for the

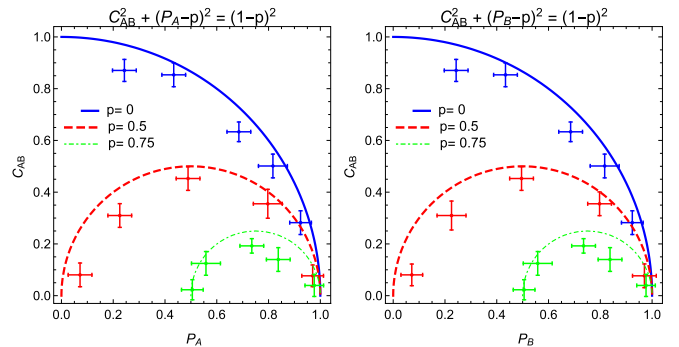


FIG. 3. Experimental tests of the constraints given on top of the graphs. The initial pure state is $|\psi_{AB}^+\rangle = \cos \theta |H_A\rangle |V_B\rangle + \sin \theta |V_A\rangle |H_B\rangle$. For $p = 0$ (state remains pure), curves were parametrized with θ taking the values $\theta = 7.00^\circ, 14.75^\circ, 22.50^\circ, 30.25^\circ, \text{ and } 38.00^\circ$. For $p = 0.5$ and $p = 0.75$, the values were $\theta = 10.00^\circ, 27.50^\circ, 45.00^\circ, 62.50^\circ, \text{ and } 80.00^\circ$.

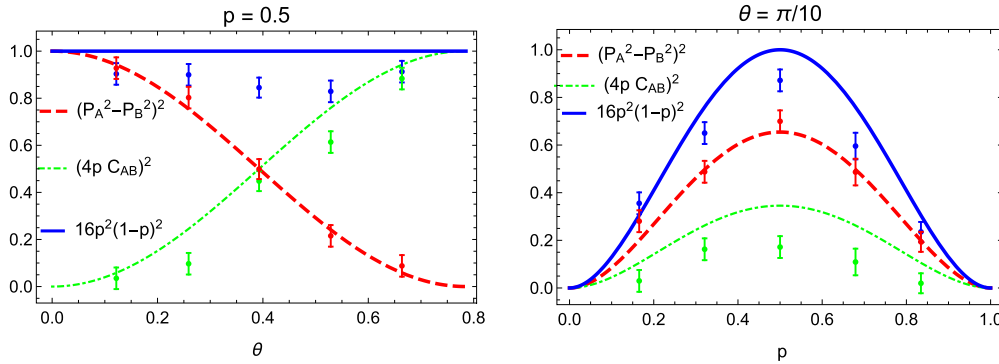


FIG. 4. Experimental test of the constraint given by Eq. (27) in the text. Left: Parameter p is held fixed, and θ , which characterizes the initial state, varies as shown in the figure. Right: Parameter θ is held fixed, and parameter p varies as shown in the figure.

mixed states into which $|\psi_{AB}^+\rangle$ evolves, when each photon is submitted to the ADC. We controlled the value of p with the half-wave plate that is set to θ_V in the Sagnac interferometers (see Fig. 1). As can be seen, our experimental results are in good agreement with theoretical predictions. Departures from the latter were as expected, due to experimental inaccuracies.

We also tested Eq. (27). We performed this test by choosing $p = 1/2$, a value for which the right-hand side of Eq. (27) is unity. Keeping p fixed, we varied θ within the range $0 \leq \theta \leq \pi/4$. Our results are displayed in the left panel of Fig. 4. Next, we addressed Eq. (27) once more, this time keeping $\theta = \pi/10$ and varying p . Our results are plotted in the right panel of Fig. 4. While our outcomes are generally in good agreement with theoretical predictions, the measured values of C_{AB} systematically lie below the theoretical curve. Most probably, this was due to imperfect alignment of some optical elements and to stray light that could not be completely blocked. In order to achieve enough stability, our interferometers had to be compact enough, which in turn put a limited margin for placement and alignment of the optical instruments. Small deviations from the intended positioning have a deleterious effect on photon entanglement. Moreover, coincident photon detections require that photon pairs remain coherent after each photon has traversed through its respective interferometer. To balance optical path lengths, we used small pieces of glass within the interferometers, with the corresponding trade-off between compactness and accessibility. Restricted access to our laboratory precluded us from improving the overall alignment and the optimization of data acquisition. Concerning the latter, we made eight measurements per plotted point. Our shortcomings notwithstanding, we consider that our results provide convincing evidence of the accordance between theory and experiment.

IV. SUMMARY AND CONCLUSIONS

In a previous work [7], it was shown that the ‘‘coherence constraint’’ $C^2 + P^2 = 1$ applies for various pairs of DOFs that characterize a transverse, optical field. For instance, if one selects polarization and transverse position, their mutual coherence is constrained by the above equality [7]. One can also take polarization and the binary path of an interferometer as the two entangled DOFs of the optical field. Again, the

same constraint holds, now referred to another coherence of the same field. Alternatively, it is possible to address a single DOF that is carried by two different objects. This is the case when we address a pair of polarization-entangled photons. In fact, the constraint $C^2 + P^2 = 1$ applies for any entangled pair of binary DOFs, no matter how these DOFs are physically realized, provided the corresponding two-qubit state is pure.

For mixed states, we should expect that the above, tight constraint relaxes into an inequality: $C^2 + P^2 \leq 1$. This inequality, and a related equality, were recently proved to hold for a subclass of so-called X states [17]. It was assumed that a pure, optical field was submitted to uncorrelated noise, as a result of which the pure state turned into a mixed state. We have addressed the same subject matter from a more general perspective, which allowed us to recover previous results and to derive new ones. We obtained three equalities that generalize the constraint $C^2 + P^2 = 1$. These equalities follow from considering the effect of the amplitude damping channel on an initial, pure two-qubit state. We showed that previous results [17] relate to the depolarizing channel and to an effective version of it. We tested our results in experiments performed with pairs of polarization-entangled photons. To the best of our knowledge, the results reported in Ref. [17] have not been tested. It is a pending task to perform the corresponding experiments, either with classical light, as proposed in Ref. [17], or in the quantum regime, as suggested by our formulation.

A point we want to emphasize is that all our results hold for two qubits, i.e., a pair of two-state systems, no matter how these qubits are physically realized. One can use classical light or single photons. What really matters is that there are two binary degrees of freedom that can be entangled. We can then deal with both entanglement and polarization and explore their interplay. It is an open question how entanglement and polarization constrain each other when the involved, two-qubit system is subjected to the influence of an environment. We have provided an answer to this question, an answer that is yet limited to X states. Hence a vast field of research remains still wide open to be explored.

ACKNOWLEDGMENT

This work was partially supported by the U.S. Office of Naval Research Global (ONR, Award No. N62909-19-1-2148, Grant No. GRANT12853637).

- [1] J. H. Eberly, X.-F. Qian, A. Al Qasimi, H. Ali, M. A. Alonso, R. Gutiérrez-Cuevas, B. J. Little, J. C. Howell, T. Malhotra, and A. N. Vamivakas, Quantum and classical optics—emerging links, *Phys. Scr.* **91**, 063003 (2016).
- [2] C. V. S. Borges, M. Hor-Meyll, J. A. O. Huguenin, and A. Z. Khoury, Bell-like inequality for the spin-orbit separability of a laser beam, *Phys. Rev. A* **82**, 033833 (2010).
- [3] K. H. Kagalwala, G. DiGiuseppe, A. F. Abouraddy, and B. E. A. Saleh, Bell's measure in classical optical coherence, *Nat. Photonics* **7**, 72 (2013).
- [4] E. Wolf, *Theory of Coherence and Polarization of Light* (Cambridge University Press, Cambridge, 2007).
- [5] A. S. M. Patoary, G. Kulkarni, and A. K. Jha, Intrinsic degree of coherence of classical and quantum states, *J. Opt. Soc. Am. B* **36**, 2765 (2019).
- [6] W. K. Wootters, Entanglement of Formation of an Arbitrary State of Two Qubits, *Phys. Rev. Lett.* **80**, 2245 (1998).
- [7] X.-F. Qian, T. Malhotra, A. N. Vamivakas, and J. H. Eberly, Coherence Constraints and the Last Hidden Optical Coherence, *Phys. Rev. Lett.* **117**, 153901 (2016).
- [8] P. Rungta, V. Buzek, C. M. Caves, M. Hillery, and G. J. Milburn, Universal state inversion and concurrence in arbitrary dimensions, *Phys. Rev. A* **64**, 042315 (2001).
- [9] X.-F. Qian, A. N. Vamivakas, and J. H. Eberly, Entanglement limits duality and vice versa, *Optica* **5**, 942 (2018).
- [10] T. Qureshi, Predictability, distinguishability and entanglement, *Opt. Lett.* **46**, 492 (2021).
- [11] A. Norrman, A. T. Friberg, and G. Leuchs, Vector-light quantum complementarity and the degree of polarization, *Optica* **7**, 93 (2020).
- [12] M. Jakob and J. A. Bergou, Quantitative complementarity relations in bipartite systems: Entanglement as a physical reality, *Opt. Commun.* **283**, 827 (2010).
- [13] B.-G. Englert, Fringe Visibility and Which-Way Information: An Inequality, *Phys. Rev. Lett.* **77**, 2154 (1996).
- [14] J. Svozilfk, A. Vallés, J. Peřina, Jr., and J. P. Torres, Revealing Hidden Coherence in Partially Coherent Light, *Phys. Rev. Lett.* **115**, 220501 (2015).
- [15] C. H. Bennett, D. P. DiVincenzo, J. Smolin, and W. K. Wootters, Mixed-state entanglement and quantum error correction, *Phys. Rev. A* **54**, 3824 (1996).
- [16] W. An-Min, Note on entanglement of an arbitrary state of two qubits, *Chin. Phys. Lett.* **17**, 243 (2000).
- [17] A. Al-Qasimi, Coherence, entanglement, and complementarity in mixed classical light, *J. Opt. Soc. Am. A* **37**, 1526 (2020).
- [18] R. F. Werner, Quantum states with Einstein-Podolsky-Rosen correlations admitting a hidden-variable model, *Phys. Rev. A* **40**, 4277 (1989).
- [19] N. Quesada, A. Al-Qasimi, and D. F. V. James, Quantum properties and dynamics of X states, *J. Mod. Opt.* **59**, 1322 (2012).
- [20] J. H. Eberly, Correlation, coherence and context, *Laser Phys.* **26**, 084004 (2016).
- [21] X.-F. Qian and J. H. Eberly, Entanglement and classical polarization states, *Opt. Lett.* **36**, 4110 (2011).
- [22] M. McLaren, T. Konrad, and A. Forbes, Measuring the non-separability of vector vortex beams, *Phys. Rev. A* **92**, 023833 (2015).
- [23] A. Aiello, F. Töppel, C. Marquardt, E. Giacobino, and G. Leuchs, Quantum-like nonseparable structures in optical beams, *New J. Phys.* **17**, 043024 (2015).
- [24] N. Sandeau, H. Akhouayri, A. Matzkin, and T. Durt, Experimental violation of Tsirelson's bound by Maxwell fields, *Phys. Rev. A* **93**, 053829 (2016).
- [25] M. H. M. Passos, W. F. Balthazar, J. Acacio de Barros, C. E. R. Souza, A. Z. Khoury, and J. A. O. Huguenin, Classical analog of quantum contextuality in spin-orbit laser modes, *Phys. Rev. A* **98**, 062116 (2018).
- [26] H. Chen, T. Peng, S. Karmakar, and Y. Shih, Simulation of Bell states with incoherent thermal light, *New J. Phys.* **13**, 083018 (2011).
- [27] B. N. Simon, S. Simon, F. Gori, M. Santarsiero, R. Borghi, N. Mukunda, and R. Simon, Nonquantum Entanglement Resolves a Basic Issue in Polarization Optics, *Phys. Rev. Lett.* **104**, 023901 (2010).
- [28] A. Luis, Coherence, polarization, and entanglement for classical fields, *Opt. Commun.* **282**, 3665 (2009).
- [29] M. A. Nielsen and I. L. Chuang, *Quantum Computation and Quantum Information* (Cambridge University Press, Cambridge, 2007).
- [30] A. Salles, F. de Melo, M. P. Almeida, M. Hor-Meyll, S. P. Walborn, P. H. Souto-Ribeiro, and L. Davidovich, Experimental investigation of the dynamics of entanglement: Sudden death, complementarity, and continuous monitoring of the environment, *Phys. Rev. A* **78**, 022322 (2008).
- [31] M. Hor-Meyll, A. Auyuanet, C. V. S. Borges, A. Aragão, J. A. O. Huguenin, A. Z. Khoury, and L. Davidovich, Environment-induced entanglement with a single photon, *Phys. Rev. A* **80**, 042327 (2009).
- [32] P. G. Kwiat, E. Waks, A. G. White, I. Appelbaum, and P. H. Eberhard, Ultrabright source of polarization-entangled photons, *Phys. Rev. A* **60**, R773 (1999).
- [33] D. F. V. James, P. G. Kwiat, W. J. Munro, and A. G. White, Measurement of qubits, *Phys. Rev. A* **64**, 052312 (2001).